Cell Communication and Signaling

RESEARCH

Open Access

ER–mitochondria contact sites regulate hepatic lipogenesis via Ip3r-Grp75-Vdac complex recruiting Seipin

Ying-Jia Chi[1†], Zhen-Yu Bai[1†], Guang-Li Feng[1], Xiao-Hong Lai[1] and Yu–Feng Song[1,2*]

Abstract

Background Mitochondria and endoplasmic reticulum (ER) contact sites (MERCS) constitute a functional communication platform for ER and mitochondria, and they play a crucial role in the lipid homeostasis of the liver. However, it remains unclear about the exact effects of MERCs on the neutral lipid synthesis of the liver.

Methods In this study, the role and mechanism of MERCS in palmitic acid (PA)-induced neutral lipid imbalance in the liver was explored by constructing a lipid metabolism animal model based on yellow catfish. Given that the structural integrity of MERCS cannot be disrupted by the si-mitochondrial calcium uniporter (si-*mcu*), the MERCS-mediated Ca^{2+} signaling in isolated hepatocytes was intercepted by transfecting them with si-*mcu* in some in vitro experiments.

Results The key findings were: (1) Hepatocellular MERCs sub-proteome analysis confirmed that, via activating Ip3r-Grp75-voltage-dependent anion channel (Vdac) complexes, excessive dietary PA intake enhanced hepatic MERCs. (2) Dietary PA intake caused hepatic neutral lipid deposition by MERCs recruiting Seipin, which promoted lipid droplet biogenesis. (3) Our findings provide the first proof that MERCs recruited Seipin and controlled hepatic lipid homeostasis, depending on Ip3r-Grp75-Vdac-controlled Ca^{2+} signaling, apart from MERCs's structural integrity. Noteworthy, our results also confirmed these mechanisms are conservative from fish to mammals.

Conclusions The findings of this study provide a new insight into the regulatory role of MERCS-recruited SEIPIN in hepatic lipid synthesis via Ip3r-Grp75-Vdac complex-mediated Ca^{2+} signaling, highlighting the critical contribution of MERCS in hepatic lipid homeostasis.

Keywords ER-mitochondria contact sites (MERCs), Hepatic lipogenesis, Seipin, Ip3r-Grp75-Vdac, Ca^{2+} Signaling

Introduction

Numerous membrane-bound and membrane-less compartmentalized organelles in eukaryotic cells are involved in multiple vital biochemical reactions [1]. It has been corroborated by accumulating evidence that these organelles are interconnected rather than isolated, to facilitate the exchange of small molecules and metabolites via membrane contact sites (MCSs) [2, 3]. These MCSs are essential for the maintenance of organelle function and homeostasis, including hepatic lipid homeostasis [4, 5]. Emerging studies indicates that a disruption in effective inter-organelle communication is strongly associated

†Ying-Jia Chi and Zhen-Yu Bai contributed equally to this work.

*Correspondence:
Yu–Feng Song
syf880310@mail.hzau.edu.cn
[1] Key Laboratory of Freshwater Animal Breeding, Ministry of Agriculture, Fishery College, Huazhong Agricultural University, Wuhan 430070, China
[2] Laboratory for Marine Fisheries Science and Food Production Processes, Qingdao National Laboratory for Marine Science and Technology, Qingdao 266237, China

with hepatic steatosis [6, 7], which is a condition characterized by an excessive buildup of neutral lipids that has rapidly spread around the world. In particular, the functional interaction between the two primary organelles (mitochondria and endoplasmic reticulum [ER]) responsible for neutral lipid metabolism has been highlighted in recent studies [8]. Palmitic acid (PA) is the most common saturated fatty acid in common diets. In the past few decades, PA-induced hepatic steatosis has been widely explored [9–11]. However, the precise molecular mechanisms through which communication between mitochondria and endoplasmic reticulum regulates PA-induced neutral lipid dysregulation and the mechanism of its involvement in hepatic steatosis have yet to be defined.

To achieve the functional interplay, ER and mitochondria communicate via mitochondria and endoplasmic reticulum contact sites (MERCS) [12], which can be regarded as the interface between the two organelles [13]. To date, the existence of MERCS has been established in various types of cells [14, 15]. These contacts have a specific structure and create microdomains that serve as a critical hub for a variety of intracellular processes [13, 16]. The first functional role associated with the MERCs compartment concerned its involvement in lipid synthesis and transfer [6, 14]. Due to the fact that MERCs are enriched in enzymes that contribute to lipid biosynthesis [16], the combined activity of endoplasmic reticulum and mitochondrial enzymes is also necessary, despite the fact that the endoplasmic reticulum is the primary organelle for lipid biosynthesis [17, 18]. Lipids must be transported from the endoplasmic reticulum to other organelles following synthesis, given these organelles are incapable of de novo phospholipid synthesis and depend exclusively on the endoplasmic reticulum as the only source [14, 16]. Consequently, the functional interplay of the endoplasmic reticulum and mitochondria during phospholipid biosynthesis and transfer is well established [19, 20]. In contrast to phospholipid metabolism, the underlying molecular mechanism for MERCS to control neutral lipid synthesis has not been sufficiently clarified, the focus of some emerging studies has been placed on the critical role of wrappER-mitochondria contacts in the very-low-density lipoprotein secretion and neutral lipid content in the liver [21, 22]. In addition, given several critical enzymes for neutral lipids synthesis are also enrich in MERCs, e.g. fatty acid CoA ligase 4 (Facl4) and diacylgycerol acyltransferase2 (Dgat2) [14, 23], implies that MERCs fulfil a great role in lipogenesis. This also suggests MERCs might be a promising target for the treatment of hepatic steatosis. Thus, additional in-depth mechanistic investigations are eagerly required.

The role of MERCs as a platform for Ca^{2+} transport is also among the most thoroughly described and proven to date [24, 25]. The endoplasmic reticulum is the principal Ca^{2+} storage organelle and has one main family of release channels to mitochondria, namely the Ip3r-Grp75-Vdac channel, which also function as a structural protein complex for MERCs [21, 26]. Briefly, Ca^{2+} efflux from the endoplasmic reticulum traverses the Ip3r-Grp75-Vdac channel across the freely permeable outer mitochondrial membrane, enters the inner mitochondrial membranes, and is accumulated by mitochondrial calcium uniporter (Mcu) [27]. As a fundamental intracellular second messenger, Ca^{2+} also plays an indispensable role in hepatic lipid homeostasis. Hence, it is necessary to examine the regulatory effect of MERCS on neutral lipid synthesis via its physical connection or relevant Ca^{2+} signaling, which may broaden the understanding of the role of MERCS in controlling neutral lipid synthesis.

Fish are the most numerous orders of vertebrates on the planet. Yellow catfish *Pelteobagrus fulvidraco*, is a freshwater teleost widely distributed in China and other countries and its whole-genome sequence information have been obtained [28]. Moreover, yellow catfish have relatively high lipid accumulation under intensive farming, making them an attractive model for studying hepatic lipid metabolism [29, 30]. Previous studies indicated the similarities in lipid metabolic processes, and regulatory pathways between yellow catfish and mammals [31, 32], suggesting yellow catfish is a good model for application to human lipid metabolism. On the other hand, palm oil, rich in PA, is considered to be an available and affordable lipid source in aquatic feed [33]. However, the PA-induced hepatic lipid accumulation has an adverse effect on aquaculture. Thus, how to reduce PA-induced excess hepatic lipid deposition is an urgent issue for fish nutritionists. We often found that during dietary PA inducing hepatic lipid accumulation always accompanied by the considerably alteration of physical interactions between endoplasmic reticulum and mitochondria in yellow catfish in our previous studies. Given liver are enriched in MERCs, to understand the role of this interaction, proteomics was used to examine the liver fractions from yellow catfish. Our results clarify systemic control mechanisms for MERCs in neutral lipids synthesis by recruiting Seipin. Importantly, the essential role of Ip3r-Grp75-voltage-dependent anion channel (Vdac) complex and their relevant Ca^{2+} signaling for MERCs recruiting Seipin and subsequent lipogenesis are revealed. These findings revealed a previously unidentified but essential role of MERCs in regulating hepatic lipid homeostasis depending on both its physical connection and relevant Ca^{2+} signaling. Furthermore, our research confirmed the similar results in the HepG2 cell

line, thereby establishing the viability of employing Ip3r-Grp75-Vdac-mediated MERCs as a preventive measure against hepatic steatosis.

Materials and methods

Ethical statement

Huazhong Agricultural University's (HZAU) institutional ethical guidelines for the care and use of laboratory animals were followed throughout all investigations, and were approved by the Ethical Committee of HZAU (identification code: Fish-2022–07-12).

Expt. 1: Animals feeding and sampling (in vivoexperiment)

We formulated six experimental diets according to recent studies [29, 30], as shown in Table S1. Since PA is easy digestible for fish [31], thus PA was taken as the lipid source, and added at the concentrations of 0 g/kg (Control group), 30 g/kg, 60 g/kg, 90 g/kg, 120 g/kg, 150 g/kg, respectively. PA was added at the expense of cellulose. As shown in Table S1, dietary lipid concentrations range from 6.62% to 13.52%. Yellow catfish feeding was determined according to our previous studies [29]. All yellow catfish (1-year-olds) were obtained from a local fish farm (Wuhan, China) and transferred into 300-L circular tanks for 2 weeks to acclimatize. During the acclimation period, all the fish were fed with specialized commercial feed for yellow catfish. At the start of the study, each tank was supplied with thirty fish of uniform size (3.47 ± 0.11 g, mean ± SEM). Each experimental diet was randomly assigned to the three water tanks, and 18 tanks were used in the experiment. The diets were fed to the fish by hand to apparent satiation twice daily (08: 30 and 16: 00 h). Fish body weights were measured every two weeks. The amount of feed consumed by the fish in each tank adopted quantitative feeding based on fish body weight and was recorded daily. Care was taken to ensure that no uneaten feed remained in the tanks during feeding. Faecal matter was also quickly removed during the experiment. Daily mortality statistics were kept. The experiment lasted for 8 weeks. During the feeding experiment, the parameters in water quality were followed: dissolved oxygen 6.49 ± 0.13 mg/L; water temperature 28.0 ± 0.5 °C; pH 7.81 ± 0.21; NH4-N 0.062 ± 0.005 mg/L.

At the end of the feeding experiment, all yellow catfish were fasted for 24 h before sampling. MS-222 was used to euthanize all of the yellow catfish. Then all yellow catfish were counted and weighed to measure survival, weight gain (WG), specific growth rate (SGR) and feed conversion rate (FCR). The morphological parameters and growth performance were shown in Table S2. The liver tissues from three fish were sampled from each tank and fixed in 4% buffered formalin or 2.5% glutaraldehyde for the subsequent observations of histology and ultrastructure. Other fish liver samples were promptly frozen in liquid nitrogen for further examination, including the contents of triglyceride, MERCs extraction, proteomic analysis, gene and protein expression. The blood was drawn from the dorsal aorta by inserting the needle between the anal fin and the caudal fin. The collected blood (3–4 ml) was chilled in ice, centrifuged at 2 °C and 3000 g for 10 min, and a sample of plasma (1-ml) was processed immediately. The extraction of PA from plasma was carried out by the method of Bilinski et al. [32] and the PA were determined by gas chromatography-mass spectrometry (GC–MS)-based analytical methods, essentially as described by Ciucanu et al. [33].

Expt. 2: Cultures and treatments of yellow catfish primary hepatocytes or HepG2 cells (in vitro experiment)

Primary hepatocyte culture and treatment: yellow catfish (3.47 ± 0.11 g, mean ± SEM) were obtained from the in vivo experiment after two weeks of acclimation. The primary hepatocytes were isolated and cultured from yellow catfish according to our recent publication [29, 30]. In order to further elucidate the underlying mechanisms of PA-enhanced MERCs mediating hepatic lipogenesis, according to our previous studies [30, 34], the cell viability in our pilot experiment (Fig. S1) we select no additional PA and 0.8 mM PA concentration incubated the primary hepatocytes. Meanwhile, based on the physiologically relevant concentrations of PA in plasma from yellow catfish (Table S3), the 0.8 mM PA concentration in vitro is closed to the physiologically relevant PA concentrations in plasma from yellow catfish after feed 150 g/kg PA diet in vivo. The cells were incubated at 28 ℃ for 48 h. Each treatment was performed in triplicate. For each cell culture, a pool of cells from three fish was used. In order to explore the role of Mcu, Grp75 and Seipin in MERCs-mediated hepatic lipid metabolism, we designed and transfected siRNA against *mcu*, *grp75* and *seipin*, respectively, to hepatocytes of yellow catfish. The inhibition efficiency of siRNA on target protein expression in this analysis are given in Fig. S2. Meanwhile, in the present study, HepG2 cells were used to identify whether there are similar results in human cell line, with the transfection of siRNA against *MCU*, *GRP75* and *SEIPIN* for human.

Sample analysis

Oil red O, Hematoxylin and Eosin (H&E), Bodipy 493/503 staining and transmission electron microscopy (TEM) observation

Oil red O and H&E staining tests were conducted according to the manufacture's instruction, and followed the description in our publication [29, 34, 35]. The ten fields of each sample were quantified by the software Image J

(NIH, Bethesda, MD, USA) to get the statistics of the relative areas of lipid droplets (LDs) in the Oil red O staining, the relative areas of vacuoles in the H&E staining.

Bodipy 493/503 staining for the LDs and TEM observation of hepatocytes were carried out according to the protocol which described in our previous publications [29, 34, 35]. The data analysis was conducted using FlowJo v.10 software.

Cell viability and determination of triglyceride

Cell viability was measured with the use of 3-(4,5-dimethylthia -zol-2-yl)-2, 5-diphenyltetrazolium bromide (V13154; Thermo Fisher Scientific) according to our previous publication [29, 34, 35]. The contents of triglyceride were determined by commercial kits (A110-1–1, Nanjing Jiancheng Bioengineering Institute), according to the manufacturer's instructions. Soluble protein content was analyzed, based on protocols by Bradford [36].

Determination of enzymatic activities

The activities of several enzymes, such as fatty acid synthase (FAS), acetyl coa carboxylase (ACC), were measured as previously described [34, 35]. The liver samples were homogenized in 0.5 mL of ice-cold buffer (0.02 M Tris–HCl, 0.25 M sucrose, 2 mM EDTA, 0.1 M sodium fluoride, 0.5 mM phenylmethyl sulphonyl fluoride, 0.01 M β-mercapto-ethanol, pH 7.4), and centrifuged at 12,000 × g at 4 ℃ for 30 min. The supernatant was collected to assay the activities of two lipogenic enzymes. FAS activity was measured with 20 mM potassium phosphate buffer (pH 6.8), 0.1 mM acetyl-CoA, 0.2 mM malonyl-CoA, and 0.5 mM NADPH. Activities of lipogenic enzymes were determined by reading the change in absorbance at 340 nm/unit of time in the reaction media. ACC activity was measured by commercial kits (BC0415, Beijing Solarbio Science & Technology).

RNA isolation and quantitative real-time PCR analysis (qPCR)

Total RNA was isolated by using the Trizol reagent and then transcribed into the cDNA by using the Reverse Transcription Kit. Analyses on gene transcript levels were conducted through the real-time quantitative PCR (qPCR) method described before [29, 34, 35]. The primer sequences used in this analysis are given in Table S3. A set of nine housekeeping genes (*gapdh, b2m, ef1α, 18 s rRNA, tuba, β-actin, hprt1, ubc9, tbp*) were selected from our transcriptome database in order to test their transcription stability. Our pilot experiment indicated that *gapdh* and *β-actin* (M = 0.27) showed the most stable levels of expression across the experimental conditions, as suggested by geNorm. Thus, the relative expression levels were normalized to the geometric mean of the combination of *gapdh* and *β-actin* and calculated using the $2^{-\Delta\Delta Ct}$ method. For siRNA experiment, the primer sequences of siRNA on target protein are given in Table S4.

Hepatocellular MERCs isolation and sub-proteome analysis

The cortical MERCs were isolated according to a previously published protocol [37]. For MERCs isolation and sub-proteome analysis, *iTRAQ* sample preparation, LC–MS/MS and data analysis was performed according to the methods described in our previous study [34, 35]. Protein lysates were obtained using lysis buffer followed by centrifugation at 12,000 rpm for 60 min at 4 °C to remove cellular debris. Protein samples (250 μg) were digested with trypsin solution over night at 37 °C and labeled with *iTRAQ* reagents according to the manufacturer's instructions. Then, typically peptides labeled with 4-plex *iTRAQ* tags were pooled and dried.

The peptides were separated on a Shimadzu LC-20AB HPLC Pump system coupled with a high pH RP column, which also been described in previous study [38]. The mass spectrometry analysis was performed as described in previous study [38], using Q-Exactive mass spectrometer (ThermoFisher Scientific, San Jose, CA), coupled with LC-20AD (Shimadzu). The software IQuant was used to quantify the labeled peptides with isobaric tags according to our previously published protocol [34, 35]. Two biological replicates were set for better coverage of the target proteome with reliable statistical consistency. All the proteins with a FDR < 1% proceeded with downstream analysis including GO, COG and Pathway. The overview of hepatocellular MERCS sub-proteome analysis was shown in Fig. S3.

Immunoprecipitation and western blot

Immunoprecipitation was performed to identify the interaction among Ip3r, Vdac1, Grp75 and Seipin based on the protocols by *Zhao* et al. [39]. Briefly, in order to conduct the immunoprecipitation analysis, we lysed the cells in NP-40 buffer (Beyotime, Nantong, China, p0013F) with the addition of a protease inhibitor cocktail (Beyotime, Nantong, China, P1010). The cell lysate was then mixed with anti-Ip3r (ab264281; abcam, Cambridge, UK), anti-Grp75 (ab2799; abcam, Cambridge, UK), anti-Vdac2 (ab14734; abcam, Cambridge, UK), anti-Mcu (ab272488; abcam, Cambridge, UK) or anti-Seipin (ab106793; abcam, Cambridge, UK), respectively, as the bait protein, at 4℃ overnight. The incubation was sustained for 3 h, followed by the addition of protein A/G agarose (P2012; Beyotime, Nantong, China). The immunocomplexes were washed 5 times by PBS supplemented with PMSF protease inhibitor. Finally, the western blot analysis was performed with anti-Ip3r (ab264281; abcam, Cambridge, UK), anti-Grp75 (ab2799; abcam, Cambridge, UK), anti-Vdac2 (ab14734; abcam, Cambridge,

UK), anti-Mcu (ab272488; abcam, Cambridge, UK) or anti-Seipin (ab106793; abcam, Cambridge, UK), as the prey protein. To identify the protein levels of Accα (PA5-17,564, Thermo Fisher Scientific, MA, US), Fas (ab128870; abcam, Cambridge, UK), Ip3r, Grp75, Vdac2, Mcu, Seipin, Cpt1, Srebp, Facl4 and Gapdh western blot analysis was performed according to our previous study [35]. Image J was used to measure the densitometry of these bands (Fig. S4).

Immunofluorescence and 2D/or 3D confocal analysis

Immunofluorescence and confocal analysis were utilized to analyze the colocalization of Seipin, Facl4, mitochondria, endoplasmic reticulum, lipid droplets, Ca^{2+} in the hepatocytes of yellow catfish, and the colocalization of Seipin, Facl4, mitochondria, endoplasmic reticulum of yellow catfish or HepG2 cells according to our most recent publications [35, 39]. For immunofluorescence analysis, the hepatocytes of yellow catfish or HepG2 cells were cultured in twelve-well plates and incubated with the corresponding treatments for 48 h, washed thrice with PBS and fixed in 4% paraformaldehyde at room temperature for 10 min, then centrifuge at 850 g for 10 min to collect the cells. Following this, they were incubated with particular primary antibodies, anti-Seipin (ab106793; abcam, Cambridge, UK), anti-Facl4 (ab227256; abcam, Cambridge, UK) (1:200), overnight at 4 °C after being blocked in 5% BSA for 2 h. Following three 5-min PBST washes, the cells were incubated for 60 min at room temperature and in the dark with a secondary anti-body made of goat anti-rabbit IgG H&L (AlexaFluor® 647, 1:500, 150,079; Abcam, MA, USA). The pictures were captured by a laser scanning confocal microscope (Leica Wetzlar, Germany). For the 3D imaging, the images were recorded by employing the Plan-Apochromat × 40 objective with a triple zoom. For mitochondria, endoplasmic reticulum, lipid droplets and Ca^{2+} confocal analysis, hepatocytes were stained by corresponding fluorescent probes, respectively, and then were captured by the laser scanning confocal microscope. The CytoFlex flow cytometer (Beckman Coulter, Miami, FL, USA) was used to measure the LDs and Ca^{2+}, which were identified as the green dots. The software FlowJo v.10 was used to analyze the data.

Statistical analysis

All data were expressed as mean ± standard error of means (SEM). The normality of data distribution and the homogeneity of variances were analyzed using the Kolmogorov–Smirnov test and Bartlett's test, respectively. Then, data were subjected to one-way ANOVA and Duncan's multiple range test using SPSS 19.0 software, and the minimum significance level was set at $P < 0.05$. Values without the same letter indicated significant difference among different treatments ($P < 0.05$); differences between si-NC and si-*seipin, grp75* or *mcu* groups were analyzed using a Student's t-test for independent samples, $^{*}P < 0.05$, $^{**}P < 0.01$.

Results

Excessive dietary PA intake caused hepatic neutral lipid accumulation mainly through de novolipogenesis

Growth performance, morphological parameters and feed utilization were shown in Table S2. The survival was 100% among the six treatments. Compared to other treatments, 120 g/kg PA and 150 g/kg PA diets significantly decreased WG and SGR, also significantly increased FCR.

In the present study, along with dietary PA intake increasing, especially in 150 g/kg PA diet group, the vacuoles in H&E, lipid droplets in Oil Red O, and triglyceride content were significantly aggravated (Fig. 1A-E). This finding suggests that excessive dietary PA intake caused hepatic lipid accumulation and dysregulation. The relative areas for triglyceride staining in the liver of the group fed 150 g/kg PA exceeded 50 percent, demonstrating the establishment of a model for hepatic steatosis. Interestingly, further studies indicated excessive dietary PA intake up-regulated the expression of genes involved in lipogenesis (enzyme: *g6pd, 6pgd, acca, fas* and *dgat2*; transcription factor: *ppary, srebp1*) and *seipin*, especially for 150 g/kg PA diet, but not lipolysis (*atgl, hsl, cpt1, pparα*) (Fig. 1F), which was further proven by the the ACC, FAS activity, the protein expression of Srebp1 and Cpt1 (Fig. 1G), implying lipogenesis might be the main

(See figure on next page.)

Fig. 1 Excessive dietary PA intake caused hepatic neutral lipid accumulation mainly through lipogenesis. **A** Representative images of yellow catfish liver tissues stained by H&E, scale bars, 50 μm, and oil red O, scale bars, 50 μm and hepatocellular ultrastructure (TEM). 200 × magnification; HE, hepatocytes; VA, vacuoles; LD, lipid droplet. **B** Relative areas for hepatic vacuoles in H&E staining. **C** Relative areas for hepatic vacuoles in oil red O staining. **D** Lipid droplet mean perimeter in TEM. **E** Hepatic triglyceride content. **F** Accα activity. **G** Fas activity. **H** Western blot analysis of Seipin, Srebp1 and Cpt1, quantitative analysis for western blot bands shown in Fig. S4. **I** The mRNA levels of genes involved in hepatic lipid homeostasis. Values are mean ± SEM ($n = 3$ represents 3 independent tanks and at least six fish were sampled from each tank). *P* value was calculated by one-way ANOVA and further post hoc Duncan's multiple range testing. Different letters (a-e) indicate significant differences among the six groups ($P < 0.05$)

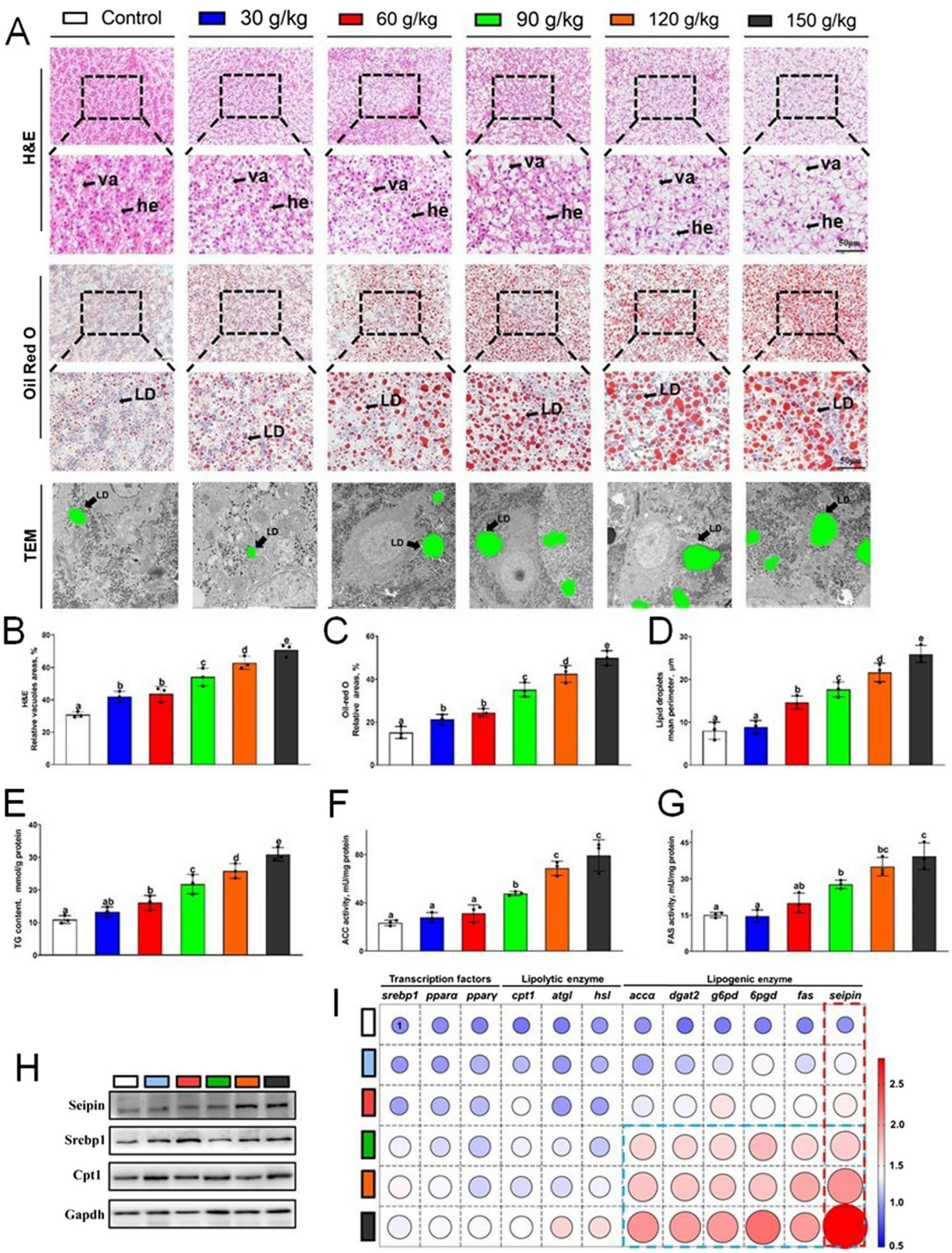

Fig. 1 (See legend on previous page.)

driving force behind excessive dietary PA intake inducing hepatic lipid accumulation. The most prominent phenotype observed among these crucial genes for lipogenesis is Seipin, which localizes at MERCs.

Dietary PA intake enhanced hepatic endoplasmic reticulum and mitochondrion contacts and MERCs structural join

Given the vital role of MERCS on hepatic lipid homeostasis, it is necessary to further identify whether dietary intake of PA can cause the structural and functional alteration of MERCS. As depicted in Fig. 2A-E, the TEM analysis results revealed that dietary intake of PA significantly decreased the contact point distance between the ER and mitochondria, while simultaneously elongating the ER-mitochondrion contact and normalizing the mitochondria perimeter. This finding suggested that dietary intake of PA promoted hepatic ER-mitochondrion contacts. Besides, dietary intake of PA significantly increased the number of extracted MERCS in the liver, indicating the activation of the structural join of MERCS.

On the other hand, the potential and pivotal role of MERCs-relevant protein on hepatic lipid metabolism has been revealed in emerging evidence [4, 6, 7]. Then, using hepatocellular MERCs sub-proteome analysis, the differentially expressed MERCS proteins were analyzed. First, overall, 13,433 unique peptides corresponding to 2325 proteins were identified. Good coverage (> 95% of the total proteins) was obtained for proteins larger than 10 kDa. MS raw files have been submitted to ProteomeXchange (accession number: 1–20,230,530-123367). Second, MERCs proteins were highly specialized in MERCs tethering, MERCS-related lipid metabolism and MERCs Ca^{2+} signaling, which is consistent with their known functions (Fig. 2F-H). Among these differentially expressed MERCs proteins involved in lipid metabolism, excessive PA diet upregulated Seipin protein expression by more than twofold, which shown the most prominent phenotype. Concerning Ca^{2+} signaling, an increased PA diet resulted in upregulation of Ip3r, Grp75, and Vdac1 by more than 1.5-fold, suggesting the activation of Ip3r/Grp75/Vdac-controlled Ca^{2+} signaling. The alteration of MERCs proteins was further verified by Western blotting (Fig. 2I).

The formation of Ip3r-Grp75-Vdac complexes but not their relevant Ca^{2+} signaling determine the integrity of MERCs

It was demonstrated that excessive dietary intake of PA caused the enrichment of SEIPIN and the activation of Ip3r/Grp75/Vdac signaling at MERCS. On that basis, the regulatory relationship between MERCS-related Ip3r/Grp75/Vdac signaling and SEIPIN was further examined. The IP analysis results confirmed that Ip3r/Grp75/Vdac formed protein complexes (Fig. 3A-C; Fig. S5A-C). Interestingly, it was further indicated that Ip3r/Grp75/Vdac complexes had an interaction relationship with SEIPIN, which interconnected with Grp75 and SEIPIN (Fig. 3D; Fig. S5D). The subcellular localization analysis results revealed that si-*grp75* reduced the enrichment of SEIPIN induced by excessive dietary intake of PA at MERCS (Fig. 3E), suggesting the potential role of Ip3r/Grp75/Vdac signaling in the recruitment of SEIPIN by MERCS.

The structural integrity of MERCS is the cornerstone for maintaining its homeostasis and function [7–9]. Mcu, which is situated in the inner mitochondrial membrane, controlled Ca^{2+} signaling but not the structural integrity of MERCs [23, 27]. Thus, si-*mcu* was designed to further examine if Ip3r/Grp75/Vdac complexes regulated MERCs recruitment Seipin by its Ca^{2+} signaling or simply by its involvement in maintaining the structural integrity of MERCs. First, si-*mcu* transfection would not influence the subcellular localization of Ip3r/Grp75/Vdac complexes into MERCs (Fig. 3E). Second, additional in vitro confocal analysis revealed that si-*grp75* compromised the structural integrity of MERCs, but si-*mcu* and si-*seipin* had no discernible impact (Fig. 4A, B), which was further confirmed by the TEM observation (Fig. 4C-G).

(See figure on next page.)

Fig. 2 Dietary PA intake enhanced hepatic endoplasmic reticulum and mitochondrion contacts and MERCs structural join. **A** Representative TEM images for hepatocellular ultrastructure and isolated MERCs. MERCs, mitochondria and endoplasmic reticulum contact sites; MT, mitochondria. **B** The contact point distance between the endoplasmic reticulum and mitochondrion in panel A. **C** The length between the endoplasmic reticulum and mitochondrion in panel A. **D** The percentage of the endoplasmic reticulum-mitochondrion contact length normalized mitochondrion perimeter. **E** The amount of MERCs number. **F** Proteins that are involved in lipid metabolism related to MERCS from the hepatocyte MERCs sub-proteome. **G** Proteins that are involved in MERCS tethering related to MERCS from the hepatocyte MERCs sub-proteome. **H** Proteins that are involved in MERCs $Ca.^{2+}$ signaling related to MERCS from the hepatocyte MERCs sub-proteome. **I** Western blot analysis of Ip3r-Grp75-Vdac1 axis and Seipin. Quantitative analysis for western blot bands shown in Fig. S4. **J** The diagram of differentially expressed MERCs protein in hepatocellular MERCs sub-proteome. Values are mean ± SEM ($n = 3$ represents 3 independent tanks and at least six fish were sampled from each tank). *P* value was calculated by one-way ANOVA and further post hoc Duncan's multiple range testing. Different letters (**a**-**e**) indicate significant differences among the six groups ($P < 0.05$)

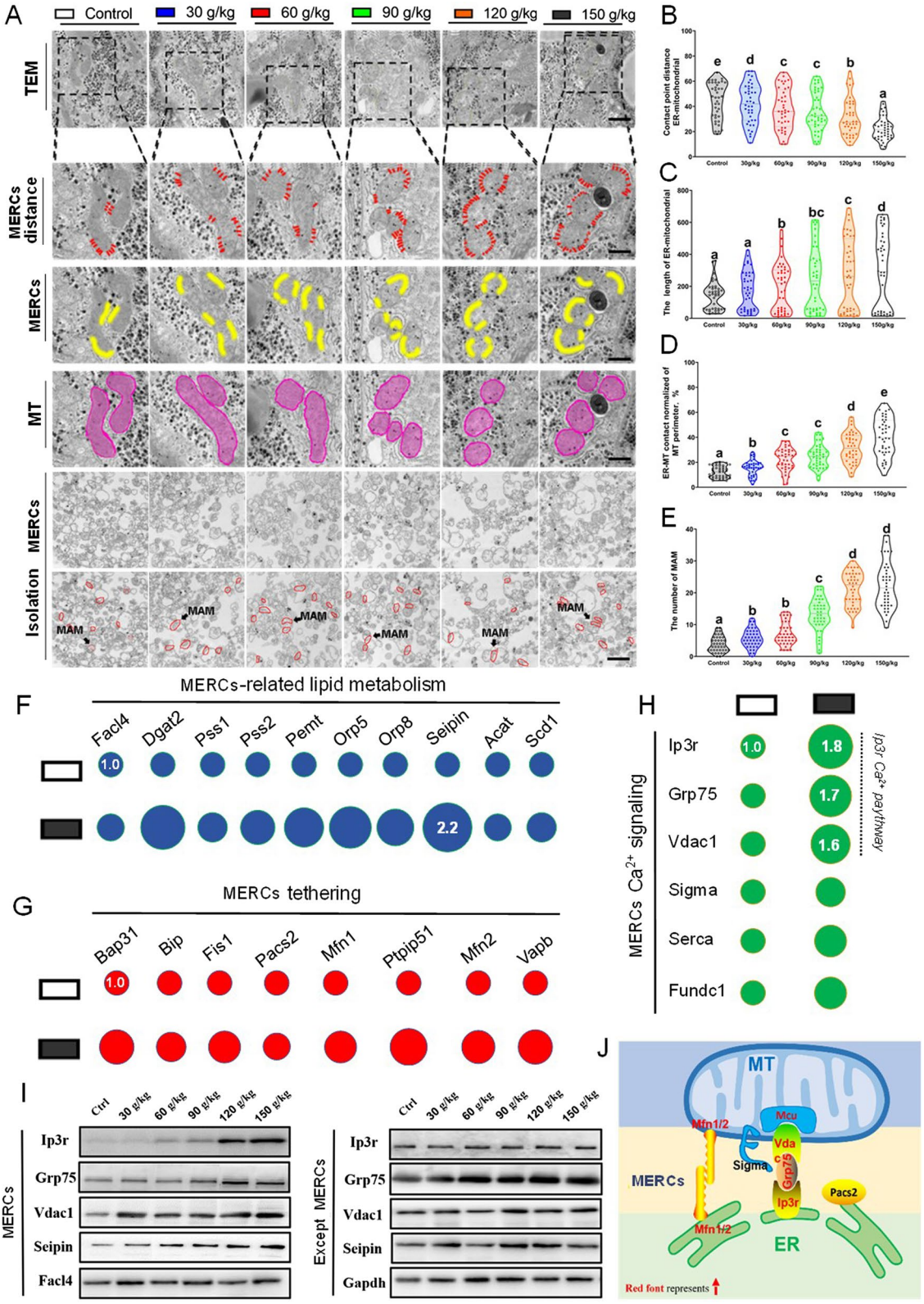

Fig. 2 (See legend on previous page.)

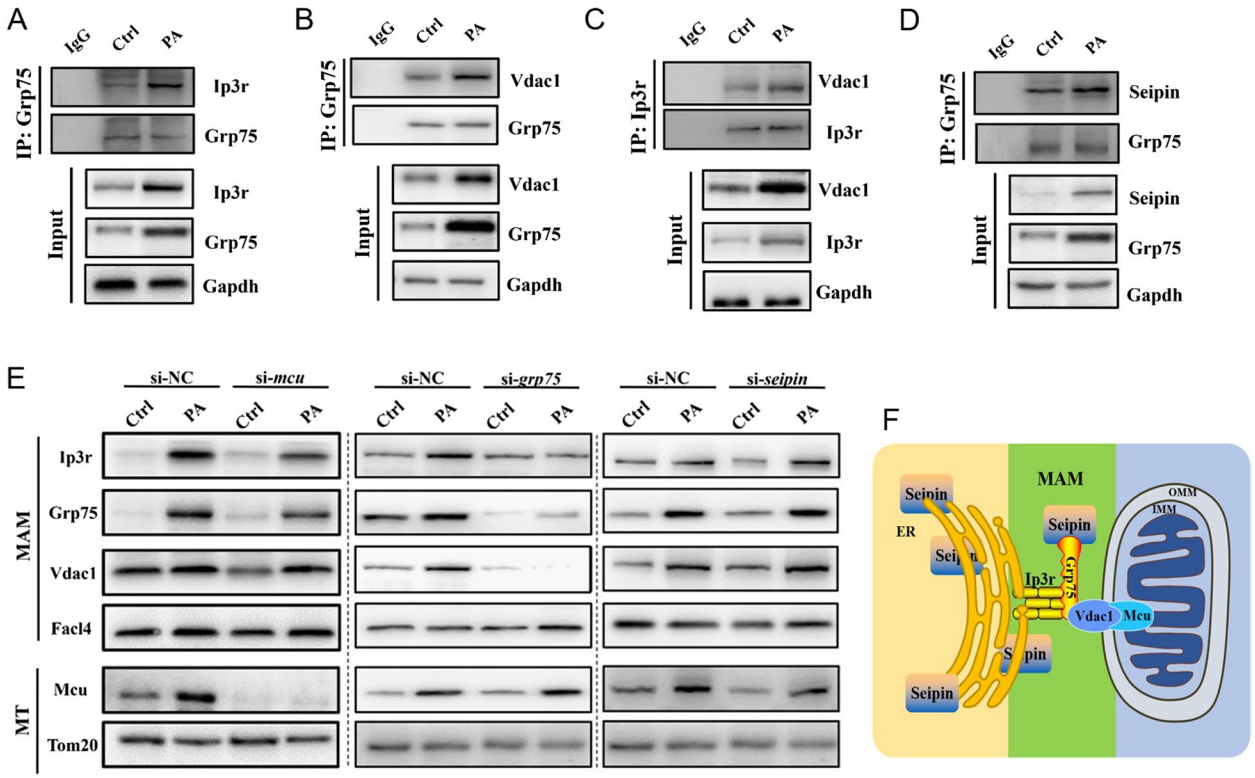

Fig. 3 The formation of Ip3r-Grp75-Vdac complexes and their correlations with Seipin and Mcu in MERCs. **A** IP analysis for Ip3r-Grp75 interaction. **B** IP analysis for Grp75-Vdac1 interaction. **C** IP analysis for Vdac1-Ip3r interaction. **D** IP analysis for Grp75-Seipin interaction. **E** Western blot analysis for subcellular localization of Ip3r, Grp75 and Vdac1 in MERCs, Mcu in mitochondrion in hepatocyte of yellow catfish with or without mcu, grp75 or seipin knockdown. Quantitative analysis for western blot bands shown in Fig. S4. **F** The diagram of Ip3r-Grp75-Vdac complexes and their correlations with Seipin and Mcu. Three independent biological experiments for all data

Ip3r-Grp75-Vdac complex and their relevant Ca^{2+} signaling is essential for MERCs recruiting Seipin

Following our previous findings that Ip3r-Grp75-Vdac complexes can regulate the structural integrity of MERCs, the mechanism by which Ip3r/Grp75/Vdac mediates MERCs recruiting Seipin was examined. Initially, subcellular localization analysis revealed, as depicted in Fig. 5A, that the down-regulation of Seipin's subcellular localization into MERCs was caused by the inhibition of both *mcu* and *grp*75. This demonstrated the critical role of the Ip3r-Grp75-Vdac complex and their respective Ca^{2+} signaling in MERCs recruiting Seipin. Co-staining with MERCS and Seipin demonstrated that the colocalization between MERCs and Seipin had diminished significantly following si-*mcu* and si-*grp*75 transfection (Fig. 5B). Altogether, these results indicated both Ip3r-Grp75-Vdac complex-maintained MERCs's structural integrity and their relevant Ca^{2+} signaling are essential for MERCs recruiting Seipin.

Ip3r-Grp75-Vdac/Mcu axis-controlled Ca^{2+} signaling and their role on the MERCs-recruited Seipin activating lipogenesis

After confirming that the Ip3r-Grp75-Vdac complex and its associated Ca^{2+} signaling play a crucial role in MERCs recruiting Seipin, more research was conducted

(See figure on next page.)

Fig. 4 Ip3r-Grp75-Vdac complex but not their relevant Ca^{2+} signaling determine the integrity of MERCs. **A** Representative confocal images of MERCS in hepatocyte staining with MT (red) and ER (green). **B** Representative 3D confocal images of MERCs in hepatocyte staining with mitochondrion (red) and endoplasmic reticulum (green). **C** Representative TEM images for hepatocellular ultrastructure in yellow catfish. scale bars, 1 μm. **D** The fusion rate between mitochondrion (red) and endoplasmic reticulum (green) in panel A. **E** The contact point distance between the endoplasmic reticulum and mitochondrion in panel C. **F** The length between the endoplasmic reticulum and mitochondrion in panel C. **G** The percentage of the endoplasmic reticulum-mitochondrion contact length normalized mitochondrion perimeter in panel C. All data were expressed as mean ± SEM ($n = 3$ represents three independent experiments, and three replicates were used for each independent experiment). *P* value was calculated by Student's t tests. Asterisk (*) indicates significant differences between two treatments ($P < 0.05$)

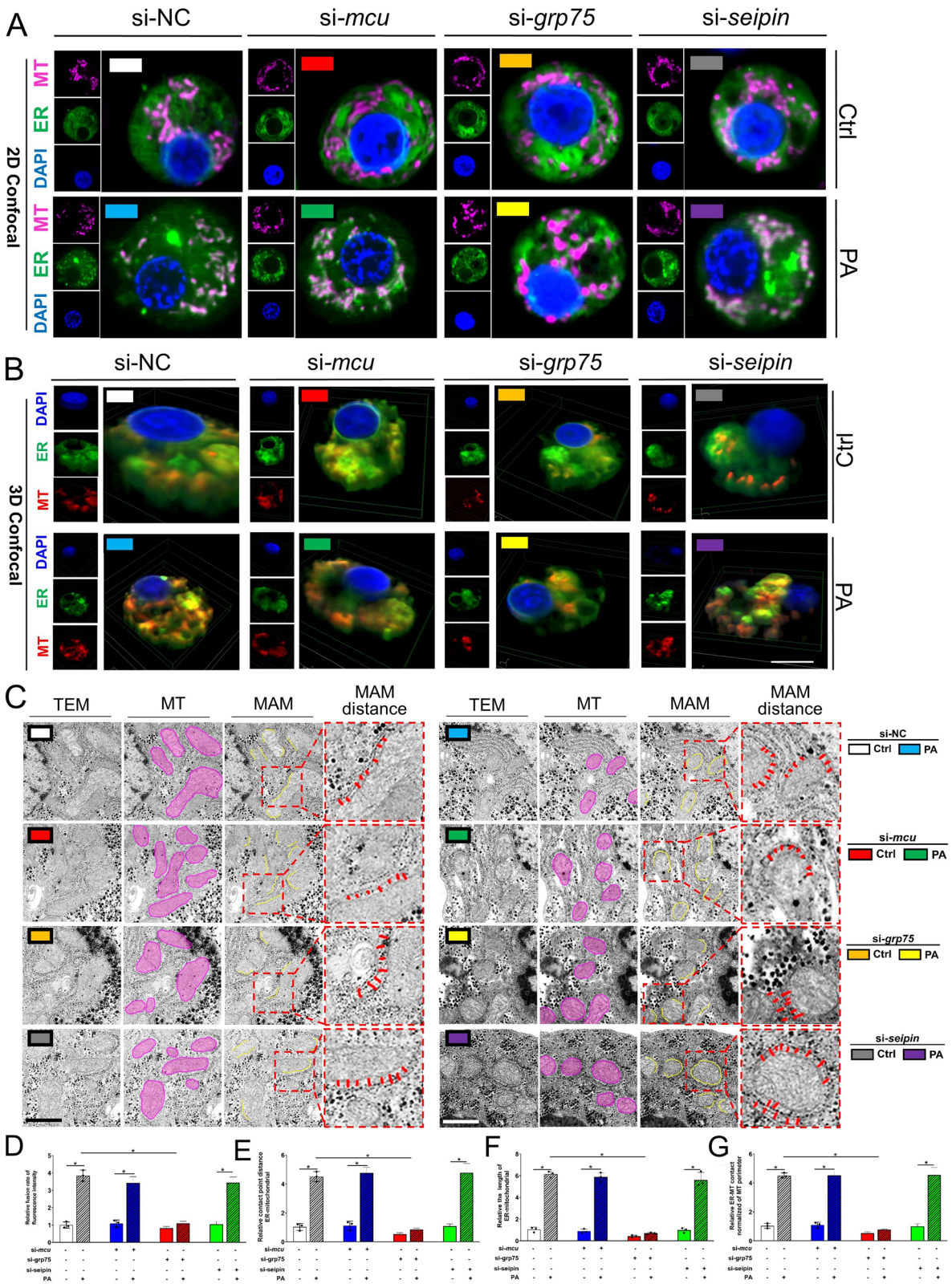

Fig. 4 (See legend on previous page.)

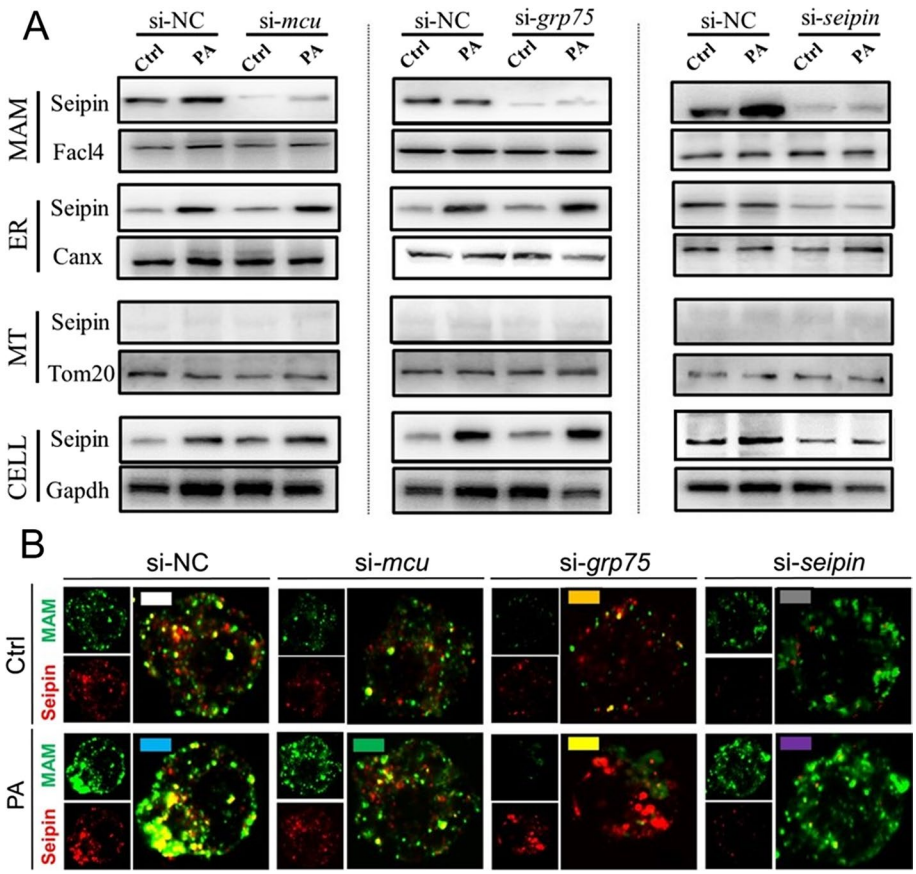

Fig. 5 Ip3r-Grp75-Vdac complex and their relevant Ca^{2+} signaling is essential for MERCs recruiting Seipin. **A** Western blot analysis for subcellular localization of Seipin in mitochondrion, endoplasmic reticulum or MERCS in hepatocyte of yellow catfish with or without mcu, grp75 or seipin knockdown. Quantitative analysis for western blot bands shown in Fig. S4. **B** Representative confocal images of co-staining between Seipin (red) and MERCs (Facl4, green) in hepatocyte of yellow catfish with or without mcu, grp75 or seipin knockdown. Three independent biological experiments for all data

to examine the effect of Ip3r-Grp75-Vdac/Mcu axis-controlled Ca^{2+} signaling on lipogenesis activated by MERCs-recruited Seipin. First, co-staining with Ca^{2+} and mitochondria clearly shown both si-*mcu* and si-*grp75* transfection decreased the mitochondrial Ca^{2+} content, suggesting the inhibition of MERCs-related Ca^{2+} signaling (Fig. 6A). Then, both si-*mcu* and si-*grp*75 reduced the accumulation of lipid droplets in hepatocytes (Fig. 6B-F) in this study, indicating that the Ip3r-Grp75-Vdac complex and its associated Ca^{2+} signaling play an upstream regulatory function in hepatic lipogenesis.

On the other hand, the aforementioned experiment was replicated using the HepG2 cell line. As illustrated in Fig. 7, the structural integrity of MERCs was not significantly impacted by si-*MCU* and si-*SEIPIN* transfection. However, si-*GRP75* transfection caused substantial damage to MERCs's structural integrity, consistent with the yellow catfish findings. Meanwhile, both si-*MCU* and si-*GRP75* transfection significantly reduced the MERCs-recruited SEIPIN. Significantly, the deposition of lipid droplets was also reduced in the down-regulated SEIPIN recruitment, further validating the central role of the Ip3r-Grp75-Vdac complex and its relevant Ca^{2+} signaling in facilitating lipogenesis through MERCs-recruited SEIPIN.

Discussion

Palmitic acid (PA) is the most common saturated fatty acid in common diets, is the most abundant saturated fatty acid. It has also emerged as a prevalent cause of hepatic steatosis [10, 40, 41], a condition primarily caused by the buildup of hepatic neutral lipid [11, 38]. In fish, as the palm oil has been widely used in aquatic feed [42], PA-induced hepatic lipid accumulation has become an adverse factor for aquaculture. Thus, understanding the induction mechanism of PA for lipid deposition also represents an urgent demand for fish nutritionists. Mitochondria and endoplasmic reticulum (ER) contact

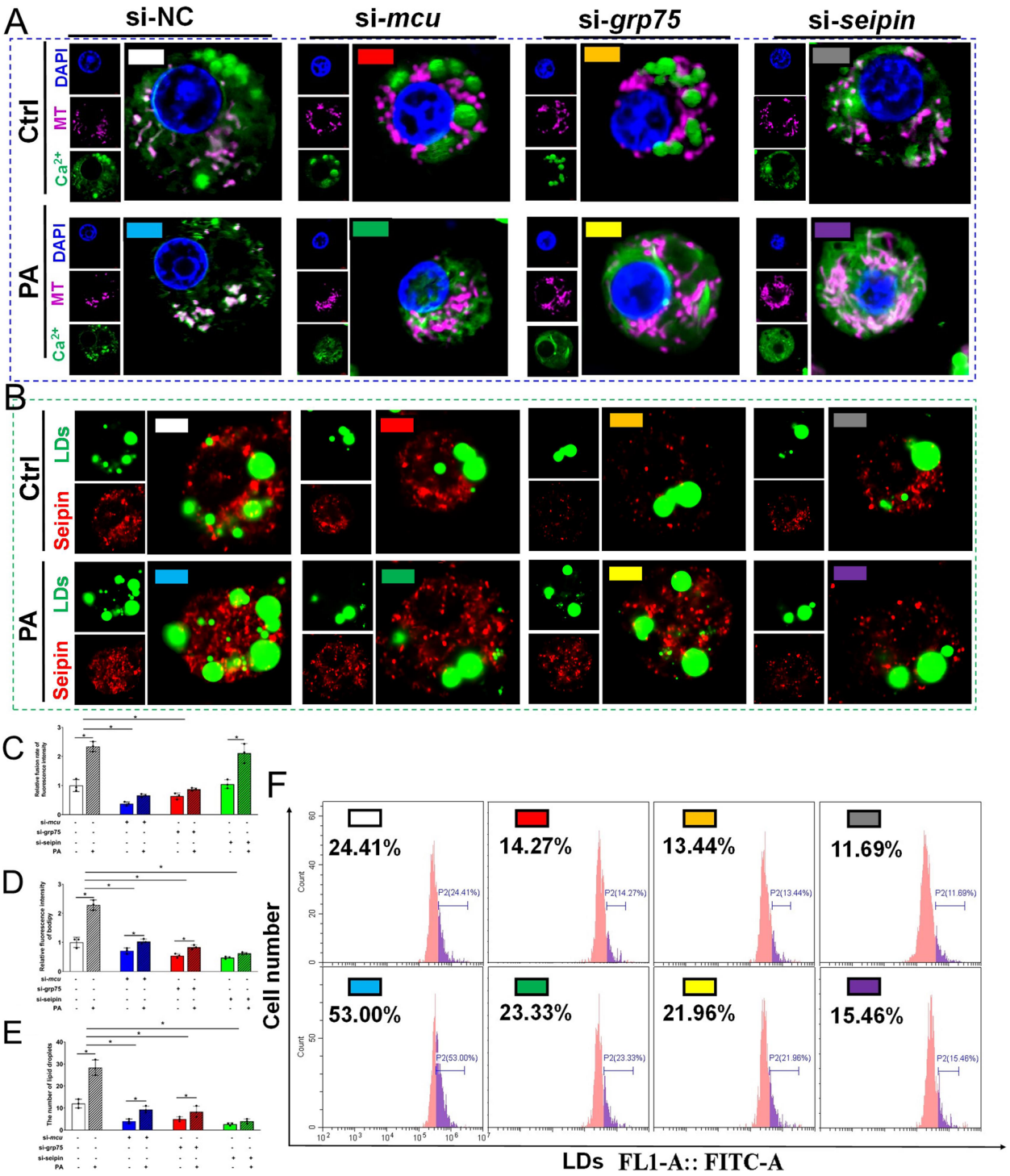

Fig. 6 Ip3r-Grp75-Vdac/Mcu axis-controlled Ca^{2+} signaling mediated MERCs-recruited Seipin to activate lipogenesis. **A** Representative confocal images of co-staining between mitochondrion (purple) and Ca^{2+} (green) in hepatocyte of yellow catfish with or without mcu, grp75 or seipin knockdown. **B** Representative confocal images of co-staining between Seipin (red) and lipid droplet (green) in hepatocyte of yellow catfish with or without mcu, grp75 or seipin knockdown. **C** Relative fusion fluorescence intensity for co-staining between MT and Ca^{2+} in panel A. **D** Relative fluorescence intensity of lipid droplet. **E** The number of lipid droplet. **F** Images of hepatocytes stained by Bodipy 493/503 (lipid droplet) output by flow cytometry analysis. All data were expressed as mean ± SEM ($n = 3$ represents three independent experiments, and three replicates were used for each independent experiment). *P* value was calculated by Student's t tests. Asterisk (*) indicates significant differences between two treatments ($P < 0.05$)

sites (MERCS) have emerged as central hubs involved in hepatic lipid homeostasis [41]. Nevertheless, the precise function of MERCs in hepatic neutral lipid production remains a subject of extensive research. Furthermore, since coordinating the Ca^{2+} transfer between the endoplasmic reticulum (ER) and the myocardium is one of the most thoroughly studied roles of the MERCs [43], it is critical to determine if the MERCS regulates hepatic lipid homeostasis through its related Ca^{2+} signaling. This study found a novel function of MERCs in hepatic neutral lipid synthesis by recruiting Seipin. Significantly, an unanticipated and crucial function for Ca^{2+} signaling associated with the Ip3r-Grp75-Vdac complex in facilitating hepatic lipogenesis activation by MERCs was discovered.

Consistent with our prior findings [30, 34], it is unsurprising that our current study unequivocally demonstrated that an excessive consumption of dietary PA resulted in the accumulation of neutral lipids in the liver, as indicated by the substantially elevated triglyceride content. This increase may be primarily attributed to increased de novo lipogenesis, not just simply up-regulation of esterification process. Amongst all dietary PA groups, 150 g/kg PA-induced hepatic lipid accumulation appears to be the most prominent phenotype, which the relative areas for triglyceride staining in liver exceeded 50%, suggesting the establishment of dietary PA-induced hepatic steatosis model in this group. MERCs are involved in many essential cellular processes and their alteration can lead to pathological conditions [44, 45]. In this regard, increasing evidence reports the dysregulation of MERCs has been associated with hepatic lipid metabolism disorder [11]. Thus, the extent to which MERCs contributes to PA-induced hepatic lipid accumulation was subsequently determined. Our research unequivocally demonstrates that liver endoplasmic reticulum-mitochondrion interactions, namely the constant, uniform distance between endoplasmic reticulum and mitochondrion, increased significantly in tandem with the increase in dietary PA concentration, thereby establishing the presence of MERCs. This observation revealed the involvement of MERCs in PA-induced hepatic neutral lipid accumulation, which is further supported by our in vitro study.

In the exploration into the mechanism of MERCS regulating hepatic lipid metabolism, our proteomics analysis clearly uncovers Seipin located at MERCs and its enrichment of Seipin at MERCs was significantly stimulated by excessive dietary PA intake in liver. As reported in previous studies suggested Seipin is a master regulator of lipid droplets biogenesis and is needed for the delivery of lipid and protein cargo to nascent lipid droplets [46]. Our further studies have shown that Seipin was mainly recruited to MERCs both in vivo and in vitro. Importantly, along with the impaired capability of MERCs recruiting Seipin, the PA-induced hepatic lipid droplets accumulation was effectively alleviated, supporting the notion that Seipin localization at MERCs is functionally relevant to PA-induced hepatic neutral lipid accumulation. In a similar manner, a recent study by Combot et al. [47] revealed that lipid loading enriches a subset of Seipin at MERCs in human and mouse cells. Additionally, the authors hypothesized that diminished mitochondrial ATP production compromises adipocyte properties in Seipin-deficient adipose tissue, thereby contributing to the pathogenesis of lipodystrophy. Recently, it has been determined that the recruitment of Seipin to MERCs-lipid droplets interactions is critical for lipid droplets biogenesis [44, 48]. According to the accumulating data, PA caused hepatic lipid metabolism disturbance by directly regulating the subcellular location of Seipin at MERCs to increase hepatic neutral lipid synthesis. In conjunction with a recent publication, these results offer unique insights into the function of MERCs-mediated Seipin [47, 48].

Which MERCs protein or protein complexes are involved in recruiting Seipin to MERCs sites? Indeed, the cross-talk between endoplasmic reticulum and mitochondrion is complex and modulated in different ways and by numerous protein complexes [13, 16, 49]. Despite the fact that numerous resident proteins at MERCs and their biological functions have been found [50–52], additional research is necessary to better comprehend the mechanism by which Seipin is recruited to MERCs. In the recent research, Yan et al. [53] discovered through resolving the structure of human Seipin that Seipin forms a scaffold that helps maintain membrane phospholipid homeostasis and ER surface tension. What's more, the integrity of ER-mitochondria contact sites is crucial for ORP5/8 function in regulating Seipin-mediated LD biogenesis [43]. These lines of evidence all pointed out that Seipin is being associated with mitochondrial and ER

(See figure on next page.)

Fig. 7 The conservative mechanisms of MERCs recruiting Seipin to activate lipogenesis via Ip3r-Grp75-Vdac complex and relevant Ca^{2+} signaling from fish to mammals. **A** HepG2 cells stained have been stained for MERCS in representative 3D confocal images with or without mcu, grp75 or seipin knockdown (nucleus, blue; MT, red; ER, green). **B** Up row: representative confocal images of co-staining between Seipin (green) and MERCs (red) in HepG2 cells with or without treatment with mcu, grp75 or seipin knockdown; Bottom row: images of hepatocytes stained by Bodipy 493/503 for lipid droplet with or without mcu, grp75 or seipin knockdown. Three independent biological experiments for all data

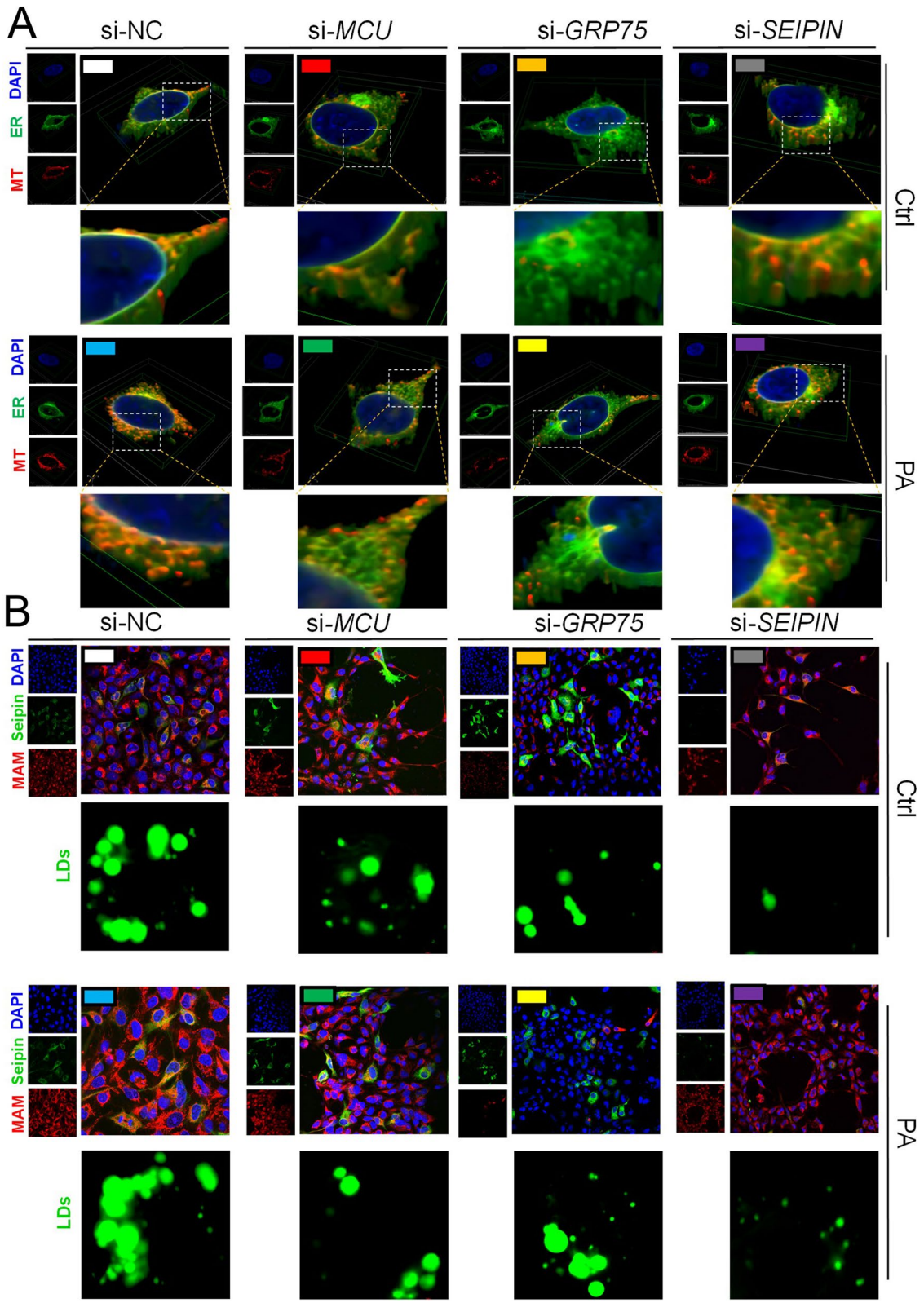

Fig. 7 (See legend on previous page.)

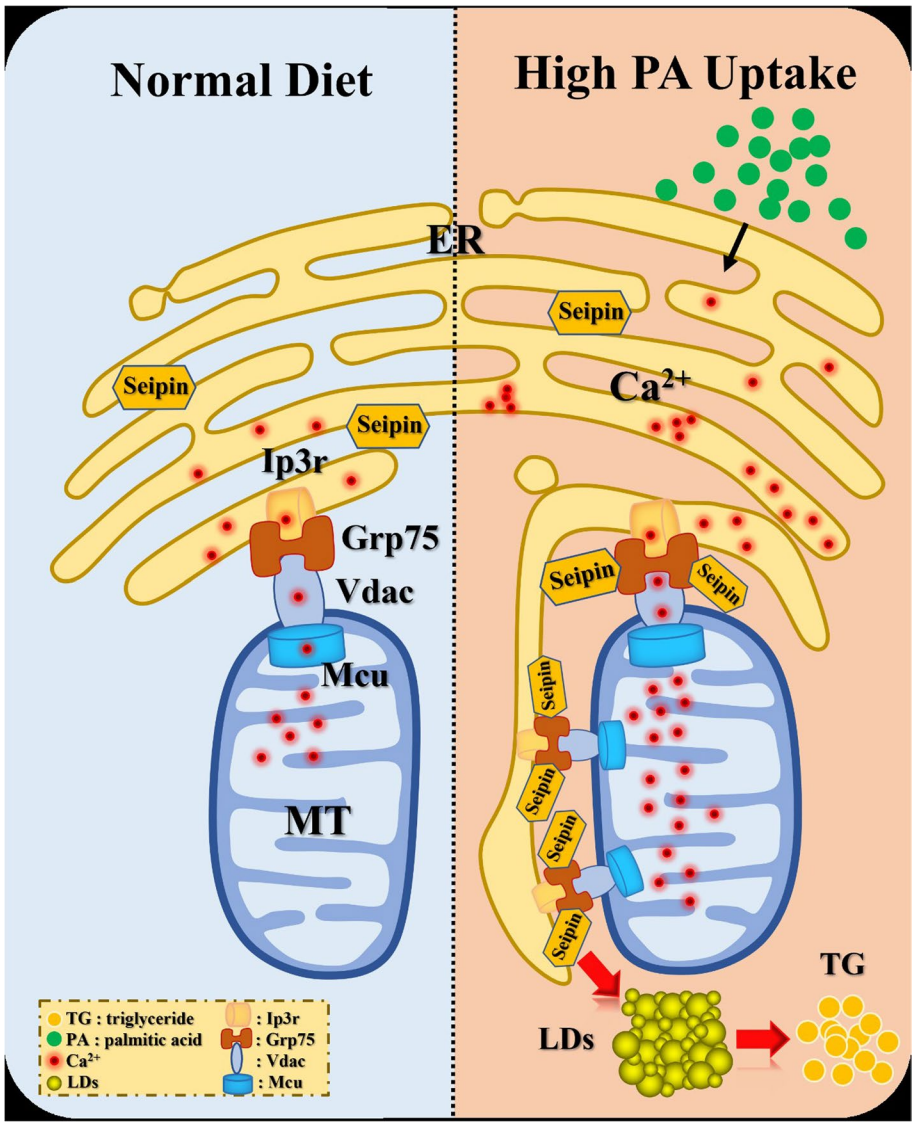

Fig. 8 Graphical conclusions for the mechanism of ER–mitochondria contact sites (MERCs) regulate hepatic lipogenesis via Ip3r-Grp75-Vdac complex recruiting Seipin in yellow catfish

functions. In the current study, MERCs was improved by the PA treatment, and our present proteomics analysis identified a clear enrichment of Ip3r-Grp75-Vdac complexes at MERCs in the liver from the excessive dietary PA group. Recent studies have highlighted the increasing importance of Ip3r-Grp75-Vdac complexes for maintaining MERCs integrity and Ca^{2+} signaling [21, 24, 25]. Our current TEM and confocal data provide further support for this notion, demonstrating that inducible deletion of Grp75 results in extended contact between the endoplasmic reticulum and mitochondrion in nearly all hepatocytes. Given the critical nature of integrity in preserving the homeostasis and functionality of MERCs, our inquiry pertains to the potential involvement of Ip3r-Grp75-Vdac complexes in the recruitment of Seipin to MERCs sites. According to our subcellular localization study and Co-IP data, Ip3r-Grp75-Vdac complexes interact directly with Seipin via Grp75-connected MERCs sites. Notably, further research proposed that the inability to subcellularly localize Seipin at MERCs sites was the consequence of Grp75 knockdown, indicating that the this Ip3r-Grp75-Vdac/Seipin interaction is crucial for MERCs recruiting Seipin. The underlying molecular mechanism of MERCs recruiting Seipin is still limited, although the recent study by Combot et al. [47] have indicated the MERCs-enriched Seipin localizes in the vicinity of

calcium regulators SERCA2, IP3R, and VDAC, further partially corroborating our data. Thus, this was the first direct evidence of MERCs recruiting Seipin via its Ip3r-Grp75-Vdac complexes.

Not only the MERCs integrity is important for MERCs recruiting Seipin, Ca^{2+} signaling also the crucial function of the Ip3r-Grp75-Vdac complexes in MERCs. The importance of MERCs in regulating Ca^{2+} transport from the endoplasmic reticulum to the mitochondrion [21, 25] has been well-documented; this is predominantly maintained through the interaction of Ip3r-Grp75-Vdac complexes. Thus, another unanswered question is Ip3r-Grp75-Vdac complexes control MERCs recruiting Seipin just though its structural functions, or also depend on its Ca^{2+} signaling? If the latter, given dysregulation of hepatic Ca^{2+} homeostasis has been linked to hepatic steatosis [54], how do Ca^{2+} signaling-mediated Seipin subcellular localization at MERCs affect hepatic lipid homeostasis? In order to address the aforementioned questions, we used the mitochondrial calcium uniporter (Mcu), a pore-forming and Ca^{2+}-conducting subunit of the uniporter holocomplex reside in the inner mitochondrial membrane (IMM), and the MERCs integrity protein Grp75. We creatively inhibited Grp75 and Mcu expression, resulting in impaired Ca^{2+} signaling and MERCs structural functions, respectively. Our confocal and TEM analyses initially validated the viability of establishing the aforementioned two distinct models: Mcu-deficient hepatocytes preserve the structural integrity of MERCs but exhibit Ca^{2+} signaling abnormalities. Notably, our study additionally discovered that inducible Mcu deletion disrupts MERCs recruiting Seipin, which eliminates the buildup of LDs. Recent research indicated that Seipin was found to physically interact with the ER calcium pump SERCA in *Drosophila*, acting as a positive SERCA regulator [55]. Further research [47] found that Seipin interacted with MERCs-enriched proteins critical for ER calcium homeostasis: SERCA2 and IP3R, and decreased mitochondrial calcium import when Seipin was acutely removed. This study linked function of Seipin to MERCs-mediated Ca^{2+} signaling. Similarly, recent studies also indicated that MERCs-recruited Seipin may play a regulatory role in regulating mitochondrial Ca^{2+} import [48], and promoted lipid storage via calcium-dependent mitochondrial metabolism [56]. What's more, Li et al. [57] also proved that Seipin regulates lipid metabolism by affecting intracellular calcium distribution. Taken together, these results reveal a novel Ca^{2+} signaling-dependent manner for MERCs recruiting Seipin and regulating hepatic lipid homeostasis, broadening and detailing the role of MERCS in lipogenesis. Significantly, the current study obtained similar results in human cell line, which further confirmed that Ip3r-Grp75-Vdac-mediated MERCs could potentially serve as a viable therapeutic target for hepatic steatosis.

In conclusion, the results of this study demonstrated that excessive consumption of dietary PA induced the recruitment of Seipin by MERCs-related Ip3r-Grp75-Vdac complexes, which then triggered lipid droplets biogenesis and ultimately resulted in hepatic steatosis. Significantly, our study also revealed an unusual method by which MERCs recruits Seipin and regulates hepatic lipid homeostasis in a manner dependent on Ca^{2+} signaling, as opposed to relying just on physical contact. A working model related to the aforementioned mechanism is shown in Fig. 8.

Abbreviations

Acc	Acetyl-CoA carboxylase
Atgl	Adipose triglyceride lipase
Cpt	Carnitine palmitoyltransferase
Dgat2	Diacylgycerol acyltransferase 2
Facl4	CoA ligase 4
FAS	FA synthase
FCR	Feed conversion rate
Grp75	75 KDa glucose-regulated protein
G6PD	Glucose 6-phosphate dehydrogenase
H&E	Hematoxylin and eosin
Hsl	Hormone sensitive lipase
Ip3r	Inositol trisphosphate receptor-1,4,5
MERCs	ER-mitochondria contact sites
MCSs	Membrane contact sites
Mcu	Mitochondrial calcium uniporter
PA	Palmitic acid
Ppar	Peroxisome proliferator-activated receptor
SGR	Specific growth rate
Srebp1	Sterol-regulator element binding protein-1
Vdac	Voltage-dependent anion channel
WG	Weight gain
6PGD	6-Phosphogluconate dehydrogenase

Supplementary Information

The online version contains supplementary material available at https://doi.org/10.1186/s12964-024-01829-x.

Supplementary Material 1.

Acknowledgements
This work was supported by the National Natural Science Foundation of China (grant No. 32273156), Biological Breeding-Major Projects (grant No. 2023ZD04054) and by Fundamental Research Funds for the Central Universities, China (grant No. 20062023SCYJ003).

Authors' contributions
Song YF designed the experiment. Chi YJ and Bai ZY conducted the experiment and data analysis with the help of Lai XH and Feng GL. Song YF drafted the manuscript. All the authors reviewed and approved the manuscript. All authors reviewed the manuscript.

Funding
National Natural Science Foundation of China (grant No. 32273156), Biological Breeding-Major Projects (grant No. 2023ZD04054) and by Fundamental Research Funds for the Central Universities, China (grant No. 20062023SCYJ003).

Availability of data and materials
The datasets in the current study are available from the corresponding author on reasonable request.

Data availability
No datasets were generated or analysed during the current study.

Declarations

Ethics approval and consent to participate
The study protocol was reviewed and approved by the Ethical Committee of Huazhong Agricultural University's (HZAU) (identification code: Fish-2022–07-12) and conformed to the ethical standards for the care and use of laboratory animals (no human subjects), as laid out in the 1964 Declaration of Helsinki and its later amendments.

Competing interests
The authors declare no competing interests.

Received: 18 July 2024 Accepted: 15 September 2024
Published online: 30 September 2024

References

1. Hirschi S, Ward TR, Meier WP, Müller DJ, Fotiadis D. Synthetic biology: bottom-up assembly of molecular systems. Chem Rev. 2022;122:16294–328.
2. Phillips MJ, Voeltz GK. Structure and function of ER membrane contact sites with other organelles. Nat Rev Mol Cell Biol. 2016;17:69–82.
3. Heeren J, Scheja L. Metabolic-associated fatty liver disease and lipoprotein metabolism. Mol Metab. 2021;50:101238.
4. Kawano Y, Cohen DE. Mechanisms of hepatic triglyceride accumulation in non-alcoholic fatty liver disease. J Gastroenterol. 2013;48:434–41.
5. Carr RM, Ahima RS. Pathophysiology of lipid droplet proteins in liver diseases. Exp Cell Res. 2016;340:187–92.
6. Rowland AA, Voeltz GK. Endoplasmic reticulum-mitochondria contacts: function of the junction. Nat Rev Mol Cell Biol. 2012;13:607–25.
7. Carreras-Sureda A, Kroemer G, Cardenas JC, Hetz C. Balancing energy and protein homeostasis at ER-mitochondria contact sites. Sci Signal. 2022;15:7524.
8. Walther TC, Farese RV Jr. Lipid droplets and cellular lipid metabolism. Annu Rev Biochem. 2012;81:687–714.
9. Fabbrini E, Magkos F. Hepatic steatosis as a marker of metabolic dysfunction. Nutrients. 2015;7:4995–5019.
10. Hardy T, Oakley F, Anstee QM, Day CP. Nonalcoholic fatty liver disease: pathogenesis and disease spectrum. Annu Rev Pathol. 2016;11:451–96.
11. Pafili K, Roden M. Nonalcoholic fatty liver disease (NAFLD) from pathogenesis to treatment concepts in humans. Mol Metab. 2021;50: 101122.
12. Biczo G, Vegh ET, Shalbueva N, Mareninova OA, Elperin J, Lotshaw E, Gretler S, Lugea A, Malla SR, Dawson D, Ruchala P, Whitelegge J, French SW, Wen L, Husain SZ, Gorelick FS, Hegyi P, Rakonczay Z Jr, Gukovsky I, Gukovskaya AS. Mitochondrial dysfunction, through impaired autophagy, leads to endoplasmic reticulum stress, deregulated lipid metabolism, and pancreatitis in animal models. Gastroenterology. 2018;154:689–703.
13. Kornmann B. The endoplasmic reticulum-mitochondria encounter structure: coordinating lipid metabolism across membranes. Biol Chem. 2020;401:811–20.
14. Arruda AP, Pers BM, Parlakgül G, Güney E, Inouye K, Hotamisligil GS. Chronic enrichment of hepatic endoplasmic reticulum-mitochondria contacts leads to mitochondrial dysfunction in obesity. Nat Med. 2014;20:1427–35.
15. Szymański J, Janikiewicz J, Michalska B, Patalas-Krawczyk P, Perrone M, Ziółkowski W, Duszyński J, Pinton P, Dobrzyń A, Więckowski MR. Interaction of Mitochondria with the Endoplasmic Reticulum and Plasma Membrane in Calcium Homeostasis, Lipid Trafficking and Mitochondrial Structure. Int J Mol Sci. 2017;18:1576.
16. Csordás G, Weaver D, Hajnóczky G. Endoplasmic Reticulum-Mitochondrial Contactology: Structure and Signaling Functions. Trends Cell Biol. 2018;28:523–40.
17. Zhong S, Li L, Liang N, Zhang L, Xu X, Chen S, Yin H. Acetaldehyde Dehydrogenase 2-regulates HMG-CoA reductase stability and cholesterol synthesis in the liver. Redox Biol. 2021;41:101919.
18. Planas-Serra L, Launay N, Goicoechea L, Heron B, Jou C, Juliá-Palacios N, Ruiz M, Fourcade S, Casasnovas C, De La Torre C, Gelot A, Marsal M, Loza-Alvarez P, García-Cazorla À, Fatemi A, Ferrer I, Portero-Otin M, Area-Gómez E, Pujol A. Sphingolipid desaturase DEGS1 is essential for mitochondria-associated membrane integrity. J Clin Invest. 2023;133:162957.
19. Monteiro JP, Oliveira PJ, Jurado AS. Mitochondrial membrane lipid remodeling in pathophysiology: a new target for diet and therapeutic interventions. Prog Lipid Res. 2013;52:513–28.
20. Yeo HK, Park TH, Kim HY, Jang H, Lee J, Hwang GS, Ryu SE, Park SH, Song HK, Ban HS, Yoon HJ, Lee BI. Phospholipid transfer function of PTPIP51 at mitochondria-associated ER membranes. EMBO Rep. 2021;22:e51323.
21. Anastasia I, Ilacqua N, Raimondi A, Lemieux P, Ghandehari-Alavijeh R, Faure G, Mekhedov SL, Williams KJ, Caicci F, Valle G, Giacomello M, Quiroga AD, Lehner R, Miksis MJ, Toth K, de Aguiar Vallim TQ, Koonin EV, Scorrano L, Pellegrini L. Mitochondria-rough-ER contacts in the liver regulate systemic lipid homeostasis. Cell Rep. 2021;34:108873.
22. Ilacqua N, Anastasia I, Aloshyn D, Ghandehari-Alavijeh R, Peluso EA, Brearley-Sholto MC, Pellegrini LV, Raimondi A, de Aguiar Vallim TQ, Pellegrini L. Expression of Synj2bp in mouse liver regulates the extent of wrappER-mitochondria contact to maintain hepatic lipid homeostasis. Biol Direct. 2022;17:37.
23. Mao H, Chen W, Chen L, Li L. Potential role of mitochondria-associated endoplasmic reticulum membrane proteins in diseases. Biochem Pharmacol. 2022;199:115011.
24. Hayashi T, Rizzuto R, Hajnoczky G, Su TP. MAM: more than just a housekeeper. Trends Cell Biol. 2009;19:81–8.
25. Horvath SE, Daum G. Lipids of mitochondria. Prog Lipid Res. 2013;52:590–614.
26. Vance JE. Phospholipid synthesis and transport in mammalian cells. Traffic. 2015;16:1–18.
27. Marchi S, Bittremieux M, Missiroli S, Morganti C, Patergnani S, Sbano L, Rimessi A, Kerkhofs M, Parys JB, Bultynck G, Giorgi C, Pinton P. Endoplasmic reticulum-mitochondria communication through Ca^{2+} signaling: the importance of Mitochondria-Associated Membranes (MAM). Adv Exp Med Biol. 2017;997:49–67.
28. Gong G, Dan C, Xiao S, Guo W, Huang P, Xiong Y, Wu J, He Y, Zhang J, Li X, Chen N, Gui JF, Mei J. Chromosomal-level assembly of yellow catfish genome using third-generation DNA sequencing and Hi-C analysis. Gigascience. 2018;7:1–9.
29. Wei CC, Wu K, Gao Y, Zhang LH, Li DD, Luo Z. Magnesium reduces hepatic lipid accumulation in yellow catfish (*Pelteobagrus fulvidraco*) and modulates lipogenesis and lipolysis via PPARA, JAK/STAT and AMPK pathways in hepatocytes. J Nutr. 2017;147:1070–8.
30. Chen G, Wu K, Zhao T, Ling SC, Liu W, Luo Z. miR-144 Mediates High Fat-Induced Changes of Cholesterol Metabolism via Direct Regulation of C/EBPα in the Liver and Isolated Hepatocytes of Yellow Catfish. J Nutr. 2010;150:464–74.
31. Ng WK, Codabaccus BM, Carter CG, Nichols PD. Replacing dietary fish oil with palm fatty acid distillate improves fatty acid digestibility in rainbow trout, oncorhynchus mykiss, maintained at optimal or elevated water temperature. Aquaculture. 2010;309:165–72.
32. Bilinski E, Gardner LJ. Effect of starvation on free fatty acid level in blood plasma and muscular tissues of rainbow trout (*Salmo gairdneri*). J Fish Res. 1968;25:1555–60.
33. Ciucanu CI, Vlad DC, Ciucanu I, Dumitrascu V. Selective and fast methylation of free fatty acids directly in plasma for their individual analysis by gas chromatography-mass spectrometry. J Chromatogr A. 2020;1625:461259.
34. Song YF, Wang LJ, Luo Z, Hogstrand C, Lai XH, Zheng FF. Moderate replacement of fish oil with palmitic acid-stimulated mitochondrial fusion promotes β-oxidation by Mfn2 interacting with Cpt1α via its GTPase-domain. J Nutr Biochem. 2024;126:109559.
35. Song YF, Gao Y, Hogstrand C, Pan YX, Luo Z. Upstream regulators of apoptosis mediates methionine-induced changes of lipid metabolism. Cell Signalling. 2018;51:176–90.
36. Bradford MM. A rapid and sensitive method for the quantitation of microgram quantities of protein utilizing the principle of protein-dye binding. Anal Biochem. 1976;72:248–54.

37. Wieckowski MR, Giorgi C, Lebiedzinska M, Duszynski J, Pinton P. Isolation of mitochondria-associated membranes and mitochondria from animal tissues and cells. Nat Protoc. 2009;4:1582–90.
38. Zhang P, Zhu S, Li Y, Zhao M, Liu M, Gao J, Ding S, Li J. Quantitative proteomics analysis to identify diffuse axonal injury biomarkers in rats using iTRAQ coupled LC-MS/MS. J Proteomics. 2016;133:93–9.
39. Zhao T, Lv WH, Hogstrand C, Zhang DG, Xu YC, Xu YH, Luo Z. Sirt3-Sod2-mROS-Mediated Manganese Triggered Hepatic Mitochondrial Dysfunction and Lipotoxicity in a Freshwater Teleost. Environ Sci Technol. 2022;56:8020–33.
40. Fabbrini E, Sullivan S, Klein S. Obesity and nonalcoholic fatty liver disease: biochemical, metabolic, and clinical implications. Hepatology. 2010;51:679–89.
41. Xiao F, Zhang J, Zhang C, An W. Hepatic stimulator substance inhibits calcium overflow through the mitochondria-associated membrane compartment during nonalcoholic steatohepatitis. Lab Invest. 2017;97:289–301.
42. Bell JG, Henderson RJ, Tocher DR, McGhee F, Dick JR, Porter A, Smullen RP, Sargent JR. Substituting fish oil with crude palm oil in the diet of Atlantic salmon (*Salmo salar*) affects muscle fatty acid composition and hepatic fatty acid metabolism. J Nutr. 2002;132:222–30.
43. Guyard V, Monteiro-Cardoso VF, Omrane M, Sauvanet C, Houcine A, Boulogne C, Ben Mbarek K, Vitale N, Faklaris O, El Khallouki N, Thiam AR. Giordano F ORP5 and ORP8 orchestrate lipid droplet biogenesis and maintenance at ER-mitochondria contact sites. J Cell Biol. 2022;221:202112107.
44. Wang WX, Prajapati P, Nelson PT, Springer JE. The Mitochondria-Associated ER Membranes Are Novel Subcellular Locations Enriched for Inflammatory-Responsive MicroRNAs. Mol Neurobiol. 2020;57:2996–3013.
45. Ponnalagu D, Hamilton S, Sanghvi S, Antelo D, Schwieterman N, Hansra I, Xu X, Gao E, Edwards JC, Bansal SS, Wold LE, Terentyev D, Janssen PML, Hund TJ, Khan M, Kohut AR, Koch WJ, Singh H. CLIC4 localizes to mitochondrial-associated membranes and mediates cardioprotection. Sci Adv. 2022;8:eabo1244.
46. Wang S, Idrissi FZ, Hermansson M, Grippa A, Ejsing CS, Carvalho P. Seipin and the membrane-shaping protein Pex30 cooperate in organelle budding from the endoplasmic reticulum. Nat Commun. 2018;9:2939.
47. Combot Y, Salo VT, Chadeuf G, Hölttä M, Ven K, Pulli I, Ducheix S, Pecqueur C, Renoult O, Lak B, Li S, Karhinen L, Belevich I, Le May C, Rieusset J, Le Lay S, Croyal M, Tayeb KS, Vihinen H, Jokitalo E, Törnquist K, Vigouroux C, Cariou B, Magré J, Larhlimi A, Ikonen E, Prieur X. Seipin localizes at endoplasmic-reticulum-mitochondria contact sites to control mitochondrial calcium import and metabolism in adipocytes. Cell Rep. 2022;38:110213.
48. Liu L, Jiang Q, Wang X, Zhang Y, Lin RC, Lam SM, Shui G, Zhou L, Li P, Wang Y, Cui X, Gao M, Zhang L, Lv Y, Xu G, Liu G, Zhao D, Yang H. Adipose-specific knockout of SEIPIN/BSCL2 results in progressive lipodystrophy. Diabetes. 2014;63:2320–31.
49. Brandenberger R, Schmidt A, Linton J, Wang D, Backus C, Denda S, Müller U, Reichardt LF. Identification and characterization of a novel extracellular matrix protein nephronectin that is associated with integrin alpha8beta1 in the embryonic kidney. J Cell Biol. 2001;154:447–58.
50. Lynes EM, Bui M, Yap MC, Benson MD, Schneider B, Ellgaard L, Berthiaume LG, Simmen T. Palmitoylated TMX and calnexin target to the mitochondria-associated membrane. EMBO J. 2012;31:457–70.
51. Wu W, Li W, Chen H, Jiang L, Zhu R, Feng D. FUNDC1 is a novel mitochondrial-associated-membrane (MAM) protein required for hypoxia-induced mitochondrial fission and mitophagy. Autophagy. 2016;12:1675–6.
52. Himms-Hagen J. Cellular thermogenesis. Annu Rev Physiol. 1976;38:315–51.
53. Yan R, Qian H, Lukmantara I, Gao M, Du X, Yan N, Yang H. Human SEIPIN Binds Anionic Phospholipids. Dev Cell. 2018;47(2):248-256.e4.
54. Maus M, Cuk M, Patel B, Lian J, Ouimet M, Kaufmann U, Yang J, Horvath R, Hornig-Do HT, Chrzanowska-Lightowlers ZM, Moore KJ, Cuervo AM, Feske S. Store-Operated Ca^{2+} Entry Controls Induction of Lipolysis and the Transcriptional Reprogramming to Lipid Metabolism. Cell Metab. 2017;25:698–712.
55. Bi J, Wang W, Liu Z, Huang X, Jiang Q, Liu G, Wang Y, Huang X. Seipin promotes adipose tissue fat storage through the ER Ca^{2+}-ATPase SERCA. Cell Metab. 2014;19(5):861–71.
56. Ding L, Yang X, Tian H, Liang J, Zhang F, Wang G, Wang Y, Ding M, Shui G, Huang X. Seipin regulates lipid homeostasis by ensuring calcium-dependent mitochondrial metabolism. EMBO J. 2018;37(17):e97572.
57. Li Q, Li Y, Zhang Z, Kang H, Zhang L, Zhang Y, Zhou L. SEIPIN overexpression in the liver may alleviate hepatic steatosis by influencing the intracellular calcium level. Mol Cell Endocrinol. 2019;488:70–8.

Publisher's Note